Biochemical Pharmacology 83 (2012) 932–940

Contents lists available at SciVerse ScienceDirect

Biochemical Pharmacology

journal homepage: www.elsevier.com/locate/biochempharm

Interplay of sorbitol pathway of glucose metabolism, 12/15-lipoxygenase, and mitogen-activated protein kinases in the pathogenesis of diabetic peripheral neuropathy

Roman Stavniichuk [a], Hanna Shevalye [a], Hiroko Hirooka [b], Jerry L. Nadler [c], Irina G. Obrosova [a,*]

[a] Pennington Biomedical Research Center, Louisiana State University System, 6400 Perkins Road, Baton Rouge, LA 70808, USA
[b] Pharmaceutical Research Laboratories, Sanwa Kagaku Kenkyusho, Mie, Japan
[c] Department of Internal Medicine, Eastern Virginia Medical School, Norfolk, VA, USA

ARTICLE INFO

Article history:
Received 30 November 2011
Accepted 12 January 2012
Available online 20 January 2012

Keywords:
Aldose reductase
Diabetic peripheral neuropathy
Dorsal root ganglion
12/15-Lipoxygenase
MAPK
Sciatic nerve
Sorbitol pathway of glucose metabolism
Spinal cord
Streptozotocin-diabetic mouse

ABSTRACT

The interactions among multiple pathogenetic mechanisms of diabetic peripheral neuropathy largely remain unexplored. Increased activity of aldose reductase, the first enzyme of the sorbitol pathway, leads to accumulation of cytosolic Ca^{2+}, essentially required for 12/15-lipoxygenase activation. The latter, in turn, causes oxidative–nitrosative stress, an important trigger of mitogen activated protein kinase (MAPK) phosphorylation. This study therefore evaluated the interplay of aldose reductase, 12/15-lipoxygenase, and MAPKs in diabetic peripheral neuropathy. In experiment 1, male control and streptozotocin-diabetic mice were maintained with or without the aldose reductase inhibitor fidarestat, 16 mg kg^{-1} d^{-1}, for 12 weeks. In experiment 2, male control and streptozotocin-diabetic wild-type (C57Bl6/J) and 12/15-lipoxygenase-deficient mice were used. Fidarestat treatment did not affect diabetes-induced increase in glucose concentrations, but normalized sorbitol and fructose concentrations (enzymatic spectrofluorometric assays) as well as 12(S)-hydroxyeicosatetraenoic concentration (ELISA), a measure of 12/15-lipoxygenase activity, in the sciatic nerve and spinal cord. 12/15-lipoxygenase expression in these two tissues (Western blot analysis) as well as dorsal root ganglia (immunohistochemistry) was similarly elevated in untreated and fidarestat-treated diabetic mice. 12/15-Lipoxygenase gene deficiency prevented diabetes-associated p38 MAPK and ERK, but not SAPK/JNK, activation in the sciatic nerve (Western blot analysis) and all three MAPK activation in the dorsal root ganglia (immunohistochemistry). In contrast, spinal cord p38 MAPK, ERK, and SAPK/JNK were similarly activated in diabetic wild-type and 12/15-lipoxygenase$^{-/-}$ mice. These findings identify the nature and tissue specificity of interactions among three major mechanisms of diabetic peripheral neuropathy, and suggest that combination treatments, rather than monotherapies, can sometimes be an optimal choice for its management.

1. Introduction

Diabetic peripheral neuropathy (DPN) affects at least 50% of patients with both Type 1 and Type 2 diabetes, and is a leading cause of foot amputation [1–3]. DPN is manifested by nerve blood flow and motor (MNCV) and sensory (SNCV) nerve conduction velocity deficits as well as by increased vibration and thermal perception thresholds that progress to sensory loss, occurring in conjunction with degeneration of all fiber types in the peripheral nerve [4]. A significant proportion of patients with DPN also describe abnormal sensations such as paresthesias, allodynia, hyperalgesia, and spontaneous pain [3–5].

The pathogenesis of DPN has extensively been studied in animal models of diabetes, and involves complex interactions between vascular and non-vascular mechanisms [6,7]. Multiple biochemical changes including, but not limited to, increased activity of the sorbitol pathway of glucose metabolism [8,9], non-enzymatic glycation/glycoxidation [10,11], activation of protein kinase C (PKC) and mitogen activated protein kinases (MAPKs) [12–15], oxidative–nitrosative stress [16–19], impaired neurotrophism [20], activation of poly(ADP-ribose) polymerase (PARP [21,22]) as well as of the enzymes of arachidonic acid metabolism, cyclooxygenase-2 [23] and 12/15-lipoxygenase (LO [24,25]), participate in the development of nerve conduction velocity deficits and small sensory nerve fiber dysfunction. Increased sorbitol pathway activity [26–28], impaired neurotrophic support [29,30], oxidative–nitrosative stress [31], PARP [32], cyclooxygenase-2 [23], and LO [25] activation have also been implicated in

* Corresponding author. Tel.: +1 225 763 0276; fax: +1 225 763 0274.
E-mail addresses: obrosoig@pbrc.edu, Irina.Obrosova@pbrc.edu (I.G. Obrosova).

0006-2952/$ – see front matter © 2012 Elsevier Inc. All rights reserved.
doi:10.1016/j.bcp.2012.01.015

axonal atrophy of large myelinated fibers and/or small sensory nerve fiber degeneration. The interactions among some of biochemical mechanisms, *e.g.* (1) increased activity of the sorbitol pathway and oxidative–nitrosative stress [8,27,28,33–35], PKC [12], p38 MAPK [14], and PARP [33] activation; (2) oxidative stress and impaired neurotrophic support [36]; (3) oxidative–nitrosative stress and PARP activation [19,32], in DPN have been identified, but many others remain largely unexplored. Diabetes-induced increase in activity of aldose reductase (AR), the first enzyme of the sorbitol pathway, has been reported to lead to accumulation of cytosolic Ca^{2+} [37], essentially required for LO activation [38,39]. The latter, in turn, causes oxidative–nitrosative stress [24], an important trigger of MAPK phosphorylation [40]. The present study therefore evaluated the interplay of AR, LO, and MAPKs in tissue sites for DPN including peripheral nerve, spinal cord, and dorsal root ganglion (DRG) neurons. The experiments were performed in C57Bl6/J mice, a robust animal model of DPN, that is manifested by MNCV and SNCV deficits, small sensory nerve fiber dysfunction and degeneration, and axonal atrophy of large myelinated fibers [9,19,24,25,27], and is amenable to treatment with AR [9,27], LO [24,41], and p38 MAPK [15] inhibitors.

2. Materials and methods

2.1. Reagents

Unless otherwise stated, all chemicals were of reagent-grade quality, and were purchased from Sigma Chemical Co., St. Louis, MO, USA. For Western blot analysis, rabbit polyclonal (clone H-100) anti-12-lipoxygenase (LO) antibody, rabbit polyclonal (clone H-147) anti-p38 MAPK antibody, mouse monoclonal anti-ERK antibody (clone MK1), rabbit polyclonal (clone C17) anti-JNK1 antibody were obtained from Santa Cruz Biotechnology, Santa Cruz, CA, USA. Rabbit polyclonal anti-phospho-p38 MAPK antibody, rabbit monoclonal (clone D13.14.4E) anti-phospho-ERK antibody, and rabbit polyclonal anti-phospho-SAPK/JNK antibody were purchased from Cell Signaling Technology, Boston, MA, USA. For immunohistochemistry, 12-lipoxygenase (murine leukocyte) polyclonal antiserum was purchased from Cayman Chemical, Ann Arbor, MI, USA. Rabbit polyclonal antibodies against p38 MAPK (clone H147), SAPK/JNK (clone FL), phospho-ERK, and phospho-SAPK/JNK were obtained from Santa Cruz Biotechnology. Rabbit polyclonal anti-ERK antibody was purchased from Abcam, Cambridge, MA, USA, and rabbit monoclonal (clone D3F9) anti-phospho-p38 MAPK antibody from Cell Signaling Technology, Boston, MA, USA. Secondary Alexa Fluor 594 goat anti-rabbit antibody, Prolong Gold Antifade Reagent, and Image-iT FX Signal Enhancer were purchased from Invitrogen, Eugene, OR, USA. VECTASHIELD Mounting Medium was obtained from Vector Laboratories, Burlingame, CA, USA.

2.2. Animals

The experiments were performed in accordance with regulations specified by the National Institutes of Health "Principles of Laboratory Animal Care, 1985 Revised Version" and Pennington Biomedical Research Center Protocol for Animal Studies. Mature C57Bl6/J mice were purchased from Jackson Laboratories. All the mice were fed standard mouse chow (PMI Nutrition International, Brentwood, MO, USA) and had *ad libitum* access to water.

In experiment 1, the mice were randomly divided into two groups. In one group, diabetes was induced by streptozotocin (STZ) as we described previously [42]. Blood samples for glucose measurements were taken from the tail vein three days after STZ injection and the day before the animals were killed. The mice with blood glucose $\geq$13.8 mM were considered diabetic. Then control and diabetic mice were maintained with or without treatment with the aldose reductase inhibitor fidarestat (SNK-860, Sanwa Kagaku Kenkyusho, Nagoya, Japan), at 16 mg kg^{-1} d^{-1} for 12 weeks.

The "leukocyte-type" 12/15-lipoxygenase-null ($LO^{-/-}$) mice were originally generated by Dr. Colin Funk, and the procedure was described in detail [43]. In Dr. Jerry Nadler's laboratory, $LO^{-/-}$ mice have been backcrossed to the B6 background for at least six generations before inbreeding for homozygosity in the experimental mice. Microsatellite testing has confirmed >96% homology between the $LO^{-/-}$ and the C57Bl6/J mice [44]. In experiment 2, a colony of $LO^{-/-}$ mice was established from several breeding pairs provided by Dr. Jerry Nadler's laboratory. Part of wild-type and $LO^{-/-}$ mice was used for induction of STZ diabetes [42]. Then non-diabetic and STZ-diabetic wild-type and $LO^{-/-}$ mice were maintained for 12 weeks.

2.3. Anesthesia, euthanasia and tissue sampling

The animals were sedated by CO_2, and immediately sacrificed by cervical dislocation. Sciatic nerves and spinal cords were rapidly dissected and frozen in liquid nitrogen for further assessment of glucose, sorbitol, fructose, LO expression, and 12(S)HETE concentrations in experiment 1, and total and phosphorylated p38 MAPK, ERK, and SAPK/JNK expression in experiment 2. Dorsal root ganglia were dissected and fixed in normal buffered 4% formalin, for subsequent evaluation of LO expression (experiment 1), and total and phosphorylated p38 MAPK, ERK, and SAPK/JNK expression in experiment 2.

2.4. Specific methods

2.4.1. Glucose and sorbitol pathway intermediates in sciatic nerve and spinal cord

Sciatic nerve and spinal cord glucose, sorbitol, and fructose concentrations were assessed by enzymatic spectrofluorometric methods with hexokinase/glucose 6-phosphate dehydrogenase, sorbitol dehydrogenase, and fructose dehydrogenase as we described in detail [45]. Measurements were taken at LS 55 Luminescence Spectrometer (PerkinElmer, MA, USA).

2.4.2. Western blot analysis of LO and total and phosphorylated p38 MAPK, ERK, and SAPK/JNK in sciatic nerve and spinal cord

To assess LO and total and phosphorylated p38 MAPK, ERK, and SAPK/JNK expression by Western blot analysis, sciatic nerve and spinal cord materials (~3–10 mg) were placed on ice in 100 μl of RIPA buffer containing 50 mmol/l Tris–HCl, pH 7.2; 150 mmol/l NaCl; 0.1% sodium dodecyl sulfate; 1% NP-40; 5 mmol/l EDTA; 1 mmol/l EGTA; 1% sodium deoxycholate and the protease/phosphatase inhibitors leupeptin (10 μg/ml), pepstatin (1 μg/ml), aprotinin (20 μg/ml), benzamidine (10 mM), phenylmethylsulfonyl fluoride (1 mM), sodium orthovanadate (1 mmol/l), and homogenized on ice. The homogenates were sonicated (4 × 10 s) and centrifuged at 14,000 × *g* for 20 min. All the aforementioned steps were performed at 4 °C. The lysates (20 and 40 μg protein for sciatic nerve and spinal cord, respectively) were mixed with equal volumes of 2× sample-loading buffer containing 62.5 mmol/l Tris–HCl, pH 6.8; 2% sodium dodecyl sulfate; 5% β-mercaptoethanol; 10% glycerol and 0.025% bromophenol blue, and fractionated in 10% (total and phosphorylated MAPKs) or 7.5% (LO) SDS-PAGE in an electrophoresis cell (Mini-Protean III; Bio-Rad Laboratories, Richmond, CA, USA). Electrophoresis was conducted at 15 mA constant current for stacking, and at 25 mA for protein separation. Gel contents were electrotransferred (80 V, 2 h) to nitrocellulose membranes using Mini Trans-Blot cell (Bio-Rad Laboratories, Richmond, CA, USA) and Western transfer buffer (10× Tris/glycine buffer, Bio-Rad Laboratories, Richmond, CA, USA) diluted with 20% (v/v) methanol. Free binding sites were blocked in 5% (w/v) BSA in

20 mmol/l Tris–HCl buffer, pH 7.5, containing 150 mmol/l NaCl and 0.05% Tween 20, for 1 h. LO and p38 MAPK, ERK, and SAPK/JNK antibodies were applied at 4 °C overnight, after which the horseradish peroxidase-conjugated secondary anti-rabbit antibody (for phosphorylated p38 MAPK, ERK, and SAPK/JNK as well as total p38 MAPK and SAPK/JNK analysis) or anti-mouse antibody (for total ERK analysis) were applied at room temperature for 1 h. After extensive washing, protein bands detected by the antibodies were visualized with the Amersham ECL™ Western Blotting Detection Reagent (Little Chalfont, Buckinghamshire, UK). Membranes were then stripped in the 25 mmol/l glycine–HCl, pH 2.5 buffer containing 2% SDS, and reprobed with β-actin antibody to confirm equal protein loading.

2.4.3. 12(S)HETE measurements

For assessment of 12(S)HETE, sciatic nerve and spinal cord samples were homogenized on ice in 15 mM Tris–HCl buffer (1:100, w/v) containing 140 mM NaCl, pH 7.6, and centrifuged. 12(S)HETE was measured in supernatants with the 12(S)-hydroxyeicosatetraenoic acid [12(S)HETE] Enzyme Immuno Assay kit (Assay Designs, Ann Arbor, MI, USA).

2.4.4. Fluorescence immunohistochemistry in dorsal root ganglia

LO and total and phosphorylated p38, ERK, and SAPK/JNK immunoreactivities in DRG neurons were assessed by immunofluorescent histochemistry. In brief, sections were deparaffinized in xylene, hydrated in decreasing concentrations of ethanol, and washed in water. All sections were processed by a single investigator and evaluated blindly. The following dilutions were used for primary antibodies: 12-LO antiserum, 1:1000; antibodies to total p38 MAPK, ERK, and SAPK/JNK, 1:50; and antibodies for phosphorylated p38 MAPK, ERK, and SAPK/JNK, 1:200. The secondary Alexa Fluor 594 goat anti-rabbit antibody was used in a working dilution 1:400. Sections were mounted in Prolong Gold Antifade Reagent. Low power observations of DRG sections stained for LO and total and phosphorylated p38 MAPK, ERK, and SAPK/JNK were made using a Zeiss Axioplan 2 imaging microscope. Color images were captured with a Photometric CoolSNAPTM HQ CCD camera at 1392 × 1040 resolution. Low power images were generated with a 40× acroplan objective using the RS ImageTM 1.9.2 software. LO and MAPK fluorescence intensity of individual DRG neurons was quantified using the ImageJ 1.43q software (National Institutes of Health, Bethesda, MD, USA), and normalized per neuronal area. 12–20 neurons per mouse were counted, and fluorescence intensity was expressed as mean ± SEM for each experimental group.

2.5. Statistical analysis

The results are expressed as mean ± SEM. Data were subjected to equality of variance F test, and then to log transformation, if necessary, before one-way analysis of variance. Where overall significance ($p < 0.05$) was attained, individual between group comparisons for multiple groups were made using the Student–Newman–Keuls multiple range test. When between-group variance differences could not be normalized by log transformation (datasets for body weights and plasma glucose), the data were analyzed by the nonparametric Kruskal–Wallis one-way analysis of variance, followed by the Bonferroni/Dunn test for multiple comparisons. Significance was defined at $p \leq 0.05$.

3. Results

3.1. Body weights and blood glucose concentrations

In experiment 1, weight gain was reduced by 14% and 18% in untreated and fidarestat-treated diabetic mice compared with controls (Table 1). Fidarestat treatment slightly (6.1%), but significantly, increased weight gain in non-diabetic mice ($p < 0.01$ *vs* untreated controls). On the contrary, weight gain in diabetic mice was slightly (4.7%), but significantly, reduced by fidarestat treatment ($p < 0.05$ *vs* untreated diabetic group). Final blood glucose concentrations were elevated by 239% and 231% in untreated and fidarestat-treated diabetic mice compared with controls. Fidarestat treatment did not affect blood glucose concentrations in either non-diabetic or diabetic mice. In experiment 2, weight gain was reduced by 28% and 38% in diabetic wild-type and diabetic $LO^{-/-}$ mice compared with the corresponding control groups. Interestingly, LO gene deficiency reduced weight gain in diabetic mice, without affecting this variable in controls. Blood glucose concentrations were similarly elevated in diabetic wild-type and diabetic $LO^{-/-}$ mice compared with the corresponding control groups.

Table 1
Body weights (g) and blood glucose concentrations (mM) in control and diabetic mice maintained with and without fidarestat treatment.

Groups	Variables	
	Body weight (g)	Blood glucose (mM)
Experiment 1		
Control	30.6 ± 0.4	7.7 ± 0.5
Control + fidarestat	32.5 ± 0.4**	8.8 ± 0.2
Diabetic	26.4 ± 0.4**	26.2 ± 1.7**
Diabetic + fidarestat	25.0 ± 0.5**,#	25.5 ± 1.4**
Experiment 2		
Control $LO^{+/+}$	40.2 ± 0.8	9.6 ± 0.2
Control $LO^{-/-}$	39.4 ± 0.8	9.9 ± 0.3
Diabetic $LO^{+/+}$	29.1 ± 0.3**	32.1 ± 0.4**
Diabetic $LO^{-/-}$	24.4 ± 0.4**,##	31.9 ± 0.4**

Data expressed as mean ± SEM. n = 10–18 per group in experiment 1, and n = 33–40 per group in experiment 2.
** $p < 0.01$ *vs* control mice.
# $p < 0.05$ *vs* diabetic mice.
$p < 0.01$ *vs* diabetic mice.

3.2. Glucose and sorbitol pathway intermediates

In experiment 1, sciatic nerve glucose, sorbitol, and fructose concentrations were increased by 290%, 344%, and 1059% in diabetic mice, compared with controls (Table 2). Fidarestat treatment did not affect sciatic nerve glucose concentrations in either control or diabetic mice. It normalized both sorbitol and fructose concentrations in diabetic mice, indicative of a complete

Table 2
Sciatic nerve and spinal cord glucose, sorbitol, and fructose concentration (nmol mg^{-1} protein) in control and diabetic mice maintained with and without fidarestat treatment.

Variables	Groups			
	Control	Control + fidarestat	Diabetic	Diabetic + fidarestat
Sciatic nerve				
Glucose	16.30 ± 1.47	18.75 ± 1.31	63.53 ± 9.04**	64.52 ± 6.84**
Sorbitol	0.27 ± 0.03	0.23 ± 0.02	1.20 ± 0.13**	0.22 ± 0.02**,##
Fructose	1.27 ± 0.50	0.23 ± 0.02	14.72 ± 0.72**	1.00 ± 0.08##
Spinal cord				
Glucose	1.38 ± 0.27	1.07 ± 0.39	8.14 ± 1.76**	7.15 ± 1.52**
Sorbitol	0.84 ± 0.06	0.79 ± 0.08	1.49 ± 0.12**	0.77 ± 0.08##
Fructose	0.83 ± 0.22	0.85 ± 0.23	1.68 ± 0.25*	0.99 ± 0.20#

Data expressed as mean ± SEM. n = 7–12 per group.
* $p < 0.05$ *vs* control mice.
** $p < 0.01$ *vs* control mice.
# $p < 0.05$ *vs* diabetic mice.
$p < 0.01$ *vs* diabetic mice.

inhibition of excessive sorbitol pathway activity. In a similar fashion, spinal cord glucose, sorbitol, and fructose concentrations were increased by 490%, 77%, and 102% in diabetic mice compared with controls. Fidarestat treatment did not affect spinal cord glucose concentrations in either control or diabetic mice. Diabetes-induced spinal cord sorbitol and fructose accumulation was completely (sorbitol) or essentially (by 83%, fructose) prevented by fidarestat.

3.3. LO expression and 12(S)HETE concentrations

Sciatic nerve and spinal cord LO expression was increased by 20% and 21%, respectively, in diabetic mice compared with controls (Fig. 1A–D). Fidarestat treatment did not affect sciatic nerve and spinal cord LO expression in either control or diabetic mice. Sciatic nerve and spinal cord 12(S)HETE concentrations, a measure of LO activity, were increased by 95% and 62% in diabetic mice compared with controls (Fig. 1E and F). Fidarestat treatment prevented diabetes-associated sciatic nerve 12(S)HETE accumulation. It reduced spinal cord 12(S)HETE accumulation to the levels that were not significantly different from those in either control ($p = 0.114$) or diabetic ($p = 0.074$) mice. LO fluorescence was similarly elevated in DRG neurons in untreated and fidarestat-treated diabetic mice compared with controls (Fig. 1G and H). Fidarestat did not affect LO fluorescence in DRG neurons of control mice.

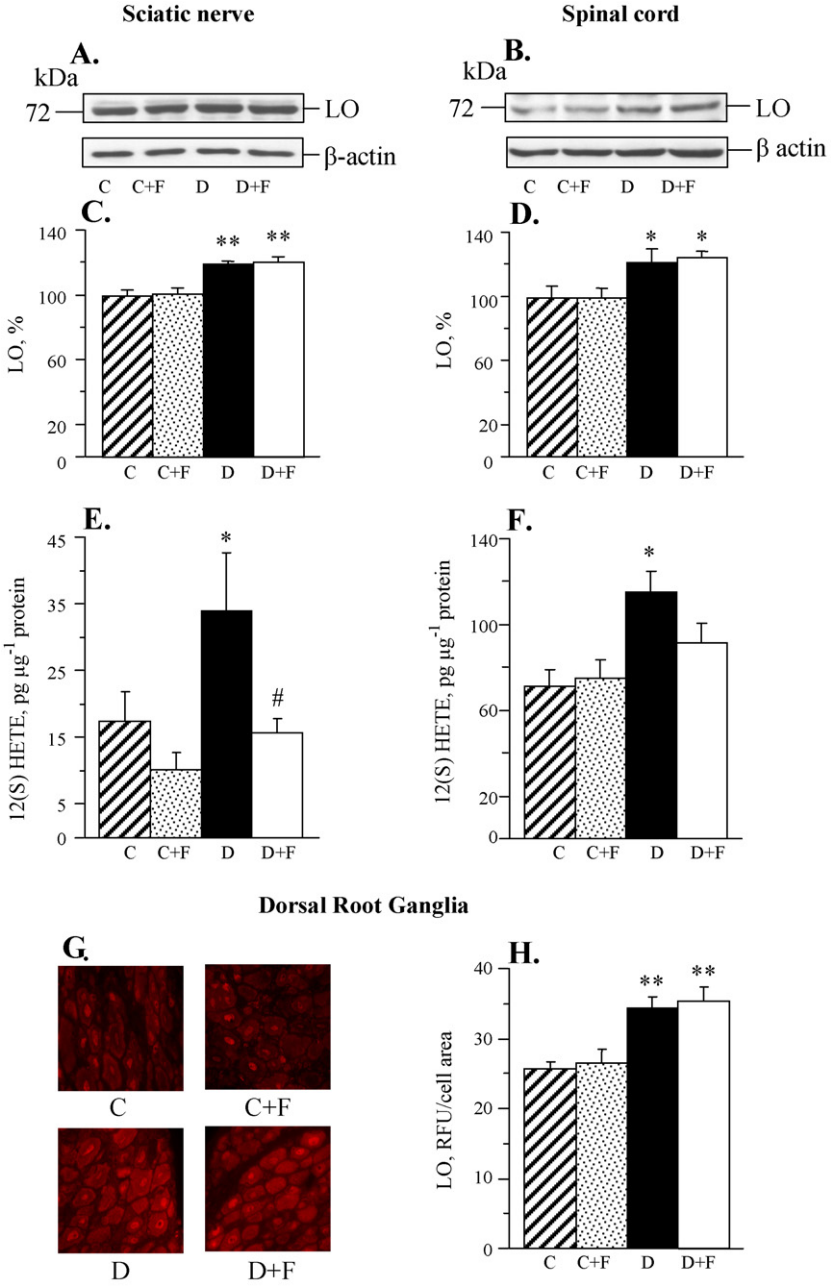

Fig. 1. Aldose reductase inhibition does not affect diabetes-induced sciatic nerve or spinal cord 12/15-lipoxygenase overexpression (A–D); essentially prevents diabetes-induced sciatic nerve 12(S)HETE accumulation and partially prevents spinal cord 12(S)HETE accumulation (E, F); and does not affect DRG 12/15-lipoxygenase overexpression (G, H). C – control group; D – diabetic group. LO – 12/15-lipoxygenase. Mean ± SEM, $n = 7–8$ per group (A–D, G, H) and $n = 7–9$ per group (E, F). $^{*}p < 0.05$, $^{**}p < 0.01$ *vs* controls. $^{\#}p < 0.05$ *vs* untreated diabetic group.

3.4. MAPK expression

Diabetic wild-type mice displayed 173%, 49%, and 44% increase in sciatic nerve p38 MAPK, ERK, and SAPK/JNK phosphorylation, compared with the corresponding control group (Fig. 2). LO gene deficiency did not affect the phosphorylation state of any of three MAPKs in non-diabetic mice. It significantly reduced p38 and ERK phosphorylation ($p < 0.05$ *vs* diabetic wild-type mice for both comparisons), but not SAPK/JNK phosphorylation, in diabetic mice. Spinal cord p38 MAPK, ERK and SAPK/JNK phosphorylation was elevated in both diabetic wild-type and diabetic $LO^{-/-}$ mice, compared with the corresponding control groups (Fig. 3). LO gene deficiency did not affect the phosphorylation state of any of three MAPKs in either non-diabetic or diabetic mice. Diabetic wild-type mice displayed 28%, 28%, and 35% increase in p38 MAPK, ERK, and SAPK/JNK phosphorylation in DRG neurons compared with the

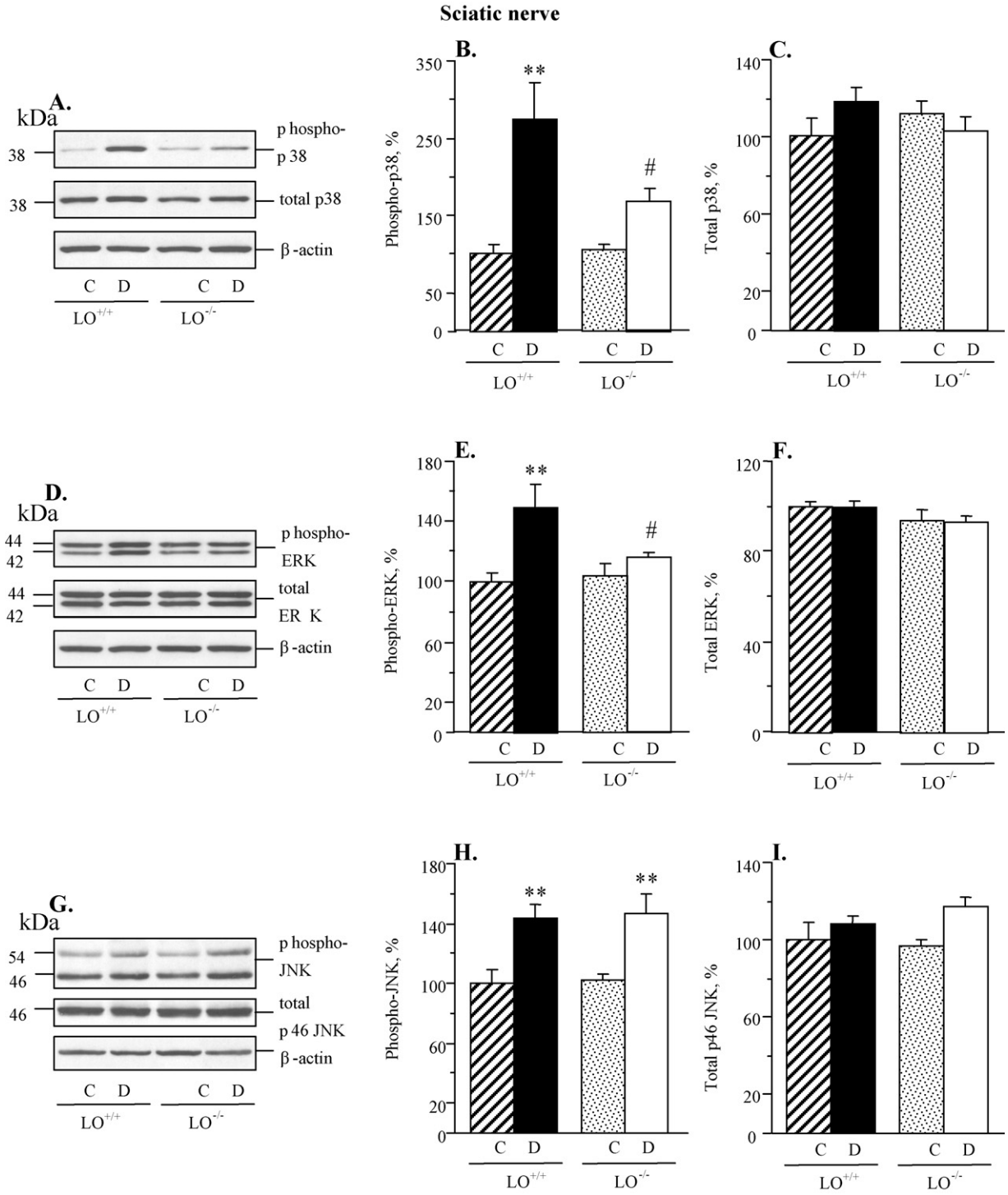

Fig. 2. 12/15-Lipoxygenase gene deficiency partially prevents diabetes-associated sciatic nerve p38 MAPK phosphorylation (A, B), essentially prevents ERK phosphorylation (D, E), and does not affect SAPK/JNK phosphorylation. (G, H) Sciatic nerve total MAPK expression was similar among the four groups (C, F, I). C – control group; D – diabetic group. LO – 12/15-lipoxygenase. Mean ± SEM, n = 8–14 per group. $^{**}p < 0.01$ *vs* controls; $^{\#}p < 0.05$ *vs* diabetic wild-type mice.

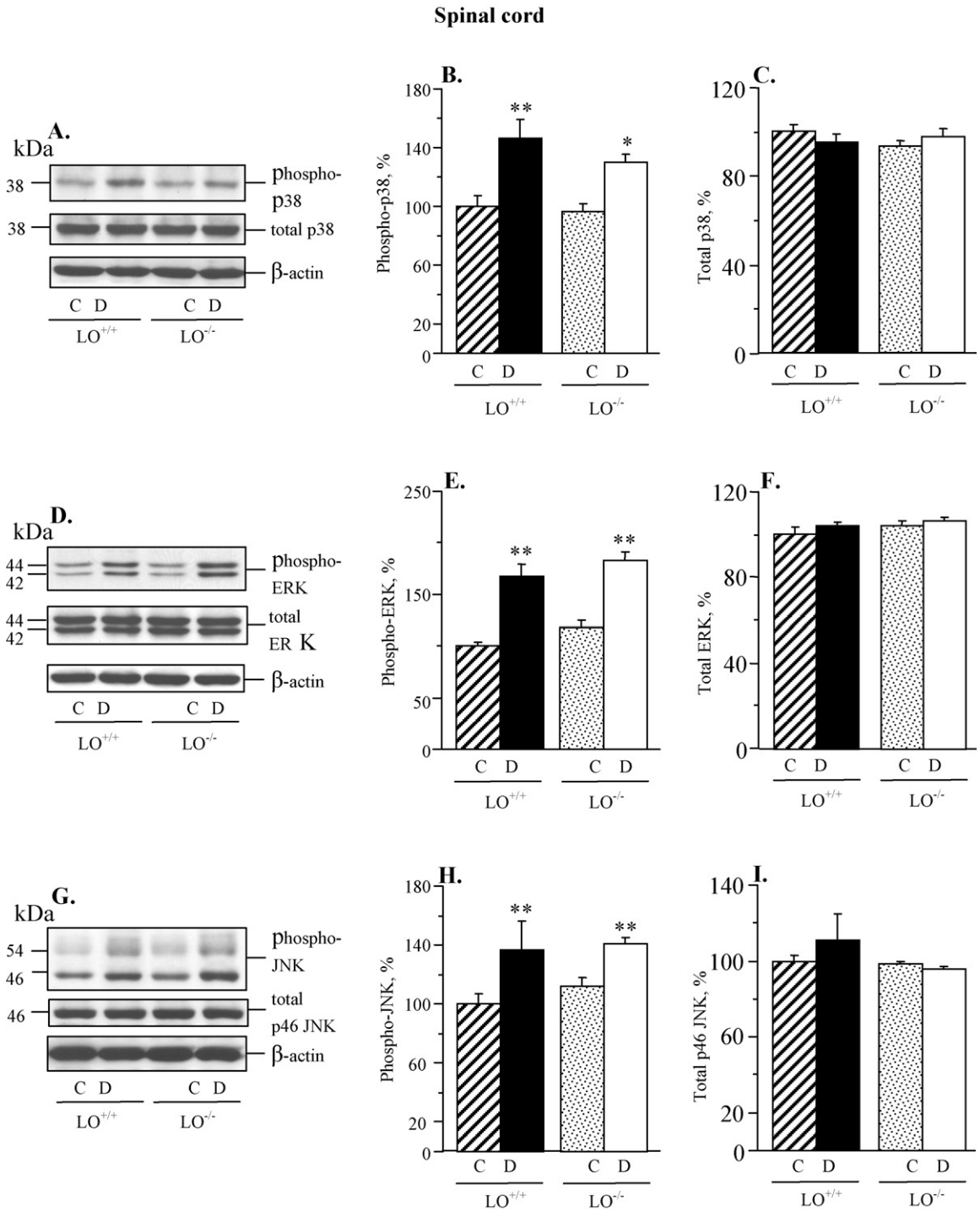

Fig. 3. 12/15-Lipoxygenase gene deficiency does not affect diabetes-induced increase in spinal cord p38 MAPK, ERK, or SAPK/JNK phosphorylation (A, B, D, E, G, H). Spinal cord total MAPK expression was similar in the four groups (A, C, D, F, G, I). C – control group; D – diabetic group. LO – 12/15-lipoxygenase. Mean ± SEM, $n = 8$ per group. $^{*}p < 0.05$, $^{**}p < 0.01$ *vs* controls.

corresponding control group (Fig. 4). LO gene deficiency reduced phosphorylation of all three MAPKs in diabetic mice, and did not affect the phosphorylation state of p38 MAPK, ERK, or JNK in non-diabetic mice.

4. Discussion

The findings described herein identify the relationships among three major mechanisms implicated in the pathogenesis of DPN. They provide the first evidence of a key role of increased AR activity in diabetes-associated LO activation in peripheral nerve and spinal cord. They also point to LO contribution to p38 MAPK and ERK activation in the peripheral nerve and to p38 MAPK, ERK, and SAPK/JNK activation in DRG. Note, that neither diabetes-induced SAPK/JNK activation in the peripheral nerve, nor the phosphorylation state of any of the three MAPKs in the spinal cord depended on LO presence and activity.

The observations of the present study are consistent with the previous reports on the presence of increased sorbitol pathway activity in peripheral nerve and spinal cord of diabetic rats

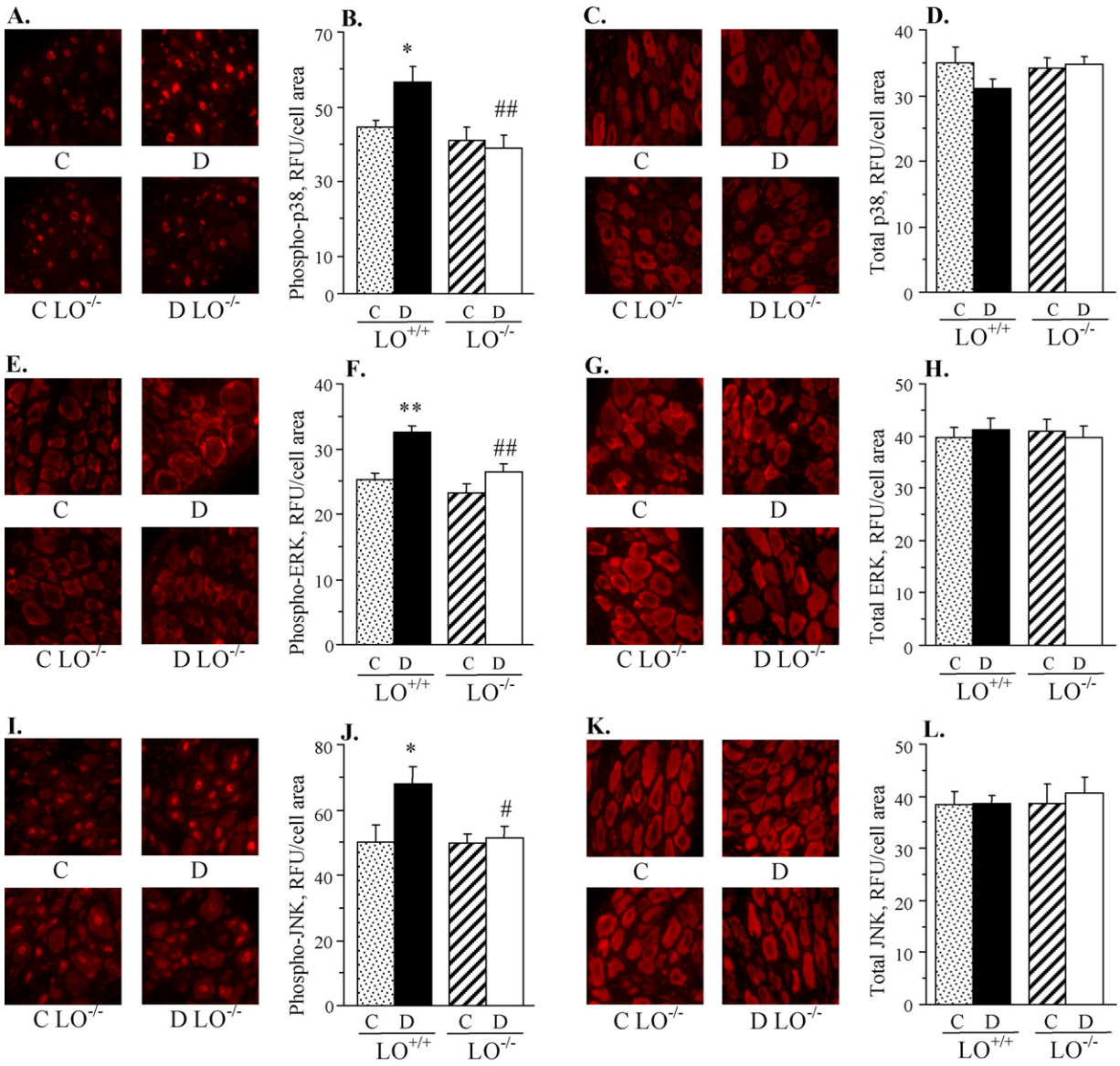

Fig. 4. 12/15-Lipoxygenase gene deficiency completely prevents diabetes-induced increase in phosphorylated p38 MAPK, ERK, and SAPK/JNK immunoreactivities in DRG (A, B, E, F, I, J). DRG total MAPK immunoreactivities were similar among the four groups (C, D, G, H, K, L). C – control group; D – diabetic group. LO – 12/15-lipoxygenase. Mean ± SEM, $n = 5–8$ per group. $^{*}p < 0.05$, $^{**}p < 0.01$ *vs* controls. $^{\#,\#\#}p < 0.05$ and <0.01 *vs* diabetic wild-type mice.

[8,12,14,26,46] and mice [9,19,27,41], and on the important role of AR in the pathogenesis of DPN in both experimental animal models [8,9,12,26,27] and human subjects with diabetes mellitus [47–49]. The findings in DRG neurons are contradictory. One group reported that AR immunoreactivity is present in satellite, but not neuronal, cells of DRG [50]. However, these observations are in disagreement with several other reports suggesting that AR participates in diabetes-associated morphological abnormalities in DRG neurons [51–53]. Furthermore, AR activation has been linked to multiple biochemical changes in tissue sites for DPN including, but not limited to, mitochondrial and cytosolic NAD^+/NADH redox imbalances and energy deficiency [8], oxidative–nitrosative stress [8,27,33–35], nerve growth factor deficit [54], activation or inhibition of PKC [12,51], and PARP [28,33], COX-2 [55], and p38 MAPK [14] activation. The relationship between AR and several of these biochemical alterations, and, in particular, oxidative–nitrosative stress, PKC inhibition as well as PARP and p38 MAPK activation has been described for DRG neurons [14,28,34,51].

Numerous findings from our group [8,33] and others [34,35] suggest that increased sorbitol pathway activity contributes to rather than results from [56] oxidative–nitrosative stress in both neural and vascular tissues in diabetes. The mechanisms underlying the relationship between the two phenomena are not well understood, although several reports suggest that increased AR activity is involved in depletion of the major non-enzymatic antioxidants, GSH, ascorbate, and taurine [8,35,57], as well as in PARP activation [33] implicated in oxidative damage [58,59]. We previously reported that diabetes-induced GSH depletion in peripheral nerve may be mediated through p38 MAPK activation [60], an AR-dependent event [14]. Two groups implicated increased activity of the second enzyme of the sorbitol pathway, sorbitol dehydrogenase (SDH), in activation of the superoxide-generating enzyme, NAD(P)H oxidase [61,62]. Note, however, that these findings are not consistent with other reports describing (1) an important role of AR rather than SDH in DPN [46,63], and (2) exacerbation, rather than amelioration, of oxidative stress with SDH inhibition in tissues of diabetic rats [64,65]. The present study suggests that increased AR activity contributes to diabetes-associated oxidative–nitrosative stress in peripheral nerve and spinal cord through LO activation, likely mediated through

accumulation of cytosolic $[Ca^{2+}]_i$. This leads to increased formation of 12(S)HETE and a number of its lipid-like derivatives, which undergo spontaneous peroxidation [38,39] and cause oxidative–nitrosative injury in both tissues [24,41]. Note that LO protein overexpression in peripheral nerve, spinal cord, and DRG neurons of diabetic mice appeared independent of AR, thus suggesting that the latter is not involved in transcriptional regulation of LO through the interleukin-4/STAT-6 pathway [38,39]. This is an unexpected observation, considering that the interleukin-4/STAT-6 pathway requires nuclear factor-κB (NF-κB) and activator protein-1 (AP-1) for interleukin-4 promoter activity. AR inhibition has been reported to blunt high glucose-induced NF-κB activation in cultured Schwann cells [66], and both NF-κB and AP-1 activation in other cell types [67].

Increased AR activity was previously implicated in diabetes-induced peripheral nerve SAPK/JNK activation in diabetic mice [27]. This is an important observation considering that SAPK/JNK activation has also been identified in sural nerve of human subjects with diabetes mellitus [40]. In the present study, increased phosphorylation of p38 MAPK, ERK, and SAPK/JNK was detected in peripheral nerve, spinal cord, and DRG of diabetic mice, consistent with the data for DRG reported for diabetic rats by others [14,40,68]. The mechanisms underlying MAPK activation in tissue sites for DPN remain unknown, although oxidative stress was implicated in p38 MAPK and ERK, but not SAPK/JNK, activation in DRG neurons [14,40]. The present findings suggest that LO may be an important mediator in diabetes-induced p38 MAPK and ERK activation in the peripheral nerve, and p38 MAPK, ERK, and SAPK/JNK activation in DRG neurons. In contrast, peripheral nerve SAPK/JNK activation and activation of all three MAPKs in the spinal cord appeared independent of LO activity. The latter is consistent with our previous observations of relatively modest effect of LO inhibition or LO gene deficiency on diabetic sensory neuropathy [24,25], in which impaired MAPK signaling plays an important role [15].

In conclusion, the findings of the present study identify the nature and tissue specificity of interactions among three major mechanisms in the pathogenesis of DPN. They implicate increased AR activity in LO activation and 12(S)HETE accumulation in peripheral nerve and spinal cord. They also suggest that combination treatments, and, in particular, with LO inhibitors plus other agents acting on spinal cord MAPKs, rather than LO inhibitor monotherapies, could be a preferable choice for management of this devastating complication of diabetes mellitus.

Acknowledgments

The study was supported in part by the National Institutes of Health Grants DK074517, DK077141, DK081147, and the American Diabetes Association Research Grant 7-08-RA-102 (all to I.G.O.). The Cell Biology and Bioimaging Core utilized in this work is supported in part by COBRE (NIH P20 RR021945) and CNRU (NIH 1P30-DK072476) center grants from the National Institutes of Health. The authors thank Dr. Rama Natarajan for valuable help with antibodies selections.

References

[1] National Institutes of Diabetes and Digestive and Kidney Diseases, editor. Diabetes in America. 2nd ed., Bethesda, MD: NIH Publication No. 95-1468; 1995.
[2] Boulton AJ. The diabetic foot: from art to science. The 18th Camillo Golgi lecture. Diabetologia 2004;47:1343–53.
[3] Boulton AJ, Vinik AI, Arezzo JC, Bril V, Feldman EL, Freeman R, et al. Diabetic neuropathies: a statement by the American Diabetes Association. Diabetes Care 2005;28:956–62.
[4] Tesfaye S, Boulton AJ, Dyck PJ, Freeman R, Horowitz M, Kempler P, et al. Diabetic neuropathies: update on definitions, diagnostic criteria, estimation of severity, and treatments. Diabetes Care 2010;33:2285–93.
[5] Veves A, Backonja M, Malik RA. Painful diabetic neuropathy: epidemiology, natural history, early diagnosis, and treatment options. Pain Med 2008;9:660–74.
[6] Cameron NE, Eaton SE, Cotter MA, Tesfaye S. Vascular factors and metabolic interactions in the pathogenesis of diabetic neuropathy. Diabetologia 2001;44:1973–88.
[7] Obrosova IG. Diabetes and the peripheral nerve. Biochim Biophys Acta 2009;1792:931–40.
[8] Obrosova IG, Van Huysen C, Fathallah L, Cao XC, Greene DA, Stevens MJ. An aldose reductase inhibitor reverses early diabetes-induced changes in peripheral nerve function, metabolism, and antioxidative defense. FASEB J 2002;16:123–5.
[9] Yagihashi S, Yamagishi SI, Wada Ri R, Baba M, Hohman TC, Yabe-Nishimura C, et al. Neuropathy in diabetic mice overexpressing human aldose reductase and effects of aldose reductase inhibitor. Brain 2001;124:2448–58.
[10] Cameron NE, Gibson TM, Nangle MR, Cotter MA. Inhibitors of advanced glycation end product formation and neurovascular dysfunction in experimental diabetes. Ann N Y Acad Sci 2005;1043:784–92.
[11] Toth C, Rong LL, Yang C, Martinez J, Song F, Ramji N, et al. Receptor for advanced glycation end products (RAGEs) and experimental diabetic neuropathy. Diabetes 2008;57:1002–17.
[12] Nakamura J, Kato K, Hamada Y, Nakayama M, Chaya S, Nakashima E, et al. A protein kinase C-beta-selective inhibitor ameliorates neural dysfunction in streptozotocin-induced diabetic rats. Diabetes 1999;48:2090–5.
[13] Cameron NE, Cotter MA, Jack AM, Basso MD, Hohman TC. Protein kinase C effects on nerve function, perfusion, Na(+), K(+)-ATPase activity and glutathione content in diabetic rats. Diabetologia 1999;42:1120–30.
[14] Price SA, Agthong S, Middlemas AB, Tomlinson DR. Mitogen-activated protein kinase p38 mediates reduced nerve conduction velocity in experimental diabetic neuropathy: interactions with aldose reductase. Diabetes 2004;53:1851–6.
[15] Cheng HT, Dauch JR, Oh SS, Hayes JM, Hong Y, Feldman EL. p38 mediates mechanical allodynia in a mouse model of type 2 diabetes. Mol Pain 2010;19:6–28.
[16] Nagamatsu M, Nickander KK, Schmelzer JD, Raya A, Wittrock DA, Tritschler H, et al. Lipoic acid improves nerve blood flow, reduces oxidative stress, and improves distal nerve conduction in experimental diabetic neuropathy. Diabetes Care 1995;18:1160–7.
[17] Cameron NE, Tuck Z, McCabe L, Cotter MA. Effect of the hydroxyl radical scavenger, dimethylthiourea, on peripheral nerve tissue perfusion, conduction velocity and nociception in experimental diabetes. Diabetologia 2001;44:1161–9.
[18] Coppey LJ, Gellett JS, Davidson EP, Dunlap JA, Lund DD, Yorek MA. Effect of antioxidant treatment of streptozotocin-induced diabetic rats on endoneurial blood flow, motor nerve conduction velocity, and vascular reactivity of epineurial arterioles of the sciatic nerve. Diabetes 2001;50:1927–37.
[19] Obrosova IG, Mabley JG, Zsengellér Z, Charniauskaya T, Abatan OI, Groves JT, et al. Role for nitrosative stress in diabetic neuropathy: evidence from studies with a peroxynitrite decomposition catalyst. FASEB J 2005;19:401–3.
[20] Lehmann HC, Höke A. Schwann cells as a therapeutic target for peripheral neuropathies. CNS Neurol Disord Drug Targets 2010;9:801–6.
[21] Li F, Drel VR, Szabó C, Stevens MJ, Obrosova IG. Low-dose poly(ADP-ribose) polymerase inhibitor-containing combination therapies reverse early peripheral diabetic neuropathy. Diabetes 2005;54:1514–22.
[22] Obrosova IG, Xu W, Lyzogubov VV, Ilnytska O, Mashtalir N, Vareniuk I, et al. PARP inhibition or gene deficiency counteracts intraepidermal nerve fiber loss and neuropathic pain in advanced diabetic neuropathy. Free Radic Biol Med 2008;44:972–81.
[23] Kellogg AP, Wiggin TD, Larkin DD, Hayes JM, Stevens MJ, Pop-Busui R. Protective effects of cyclooxygenase-2 gene inactivation against peripheral nerve dysfunction and intraepidermal nerve fiber loss in experimental diabetes. Diabetes 2007;56:2997–3005.
[24] Stavniichuk R, Drel VR, Shevalye H, Vareniuk I, Stevens MJ, Nadler JL, et al. Role of 12/15-lipoxygenase in nitrosative stress and peripheral prediabetic and diabetic neuropathies. Free Radic Biol Med 2010;49:1036–45.
[25] Obrosova IG, Stavniichuk R, Drel VR, Shevalye H, Vareniuk I, Nadler JL, et al. Different roles of 12/15-lipoxygenase in diabetic large and small fiber peripheral and autonomic neuropathies. Am J Pathol 2010;177:1436–47.
[26] Kato N, Mizuno K, Makino M, Suzuki T, Yagihashi S. Effects of 15-month aldose reductase inhibition with fidarestat on the experimental diabetic neuropathy in rats. Diabetes Res Clin Pract 2000;50:77–85.
[27] Ho EC, Lam KS, Chen YS, Yip JC, Arvindakshan M, Yamagishi S, et al. Aldose reductase-deficient mice are protected from delayed motor nerve conduction velocity, increased c-Jun NH2-terminal kinase activation, depletion of reduced glutathione, increased superoxide accumulation, and DNA damage. Diabetes 2006;55:1946–53.
[28] Drel VR, Mashtalir N, Ilnytska O, Shin J, Li F, Lyzogubov VV, et al. The leptin-deficient (ob/ob) mouse: a new animal model of peripheral neuropathy of type 2 diabetes and obesity. Diabetes 2006;55:3335–43.
[29] Toth C, Brussee V, Zochodne DW. Remote neurotrophic support of epidermal nerve fibres in experimental diabetes. Diabetologia 2006;49:1081–8.
[30] Francis G, Martinez J, Liu W, Nguyen T, Ayer A, Fine J, et al. Intranasal insulin ameliorates experimental diabetic neuropathy. Diabetes 2009;58:934–45.
[31] Sagara M, Satoh J, Wada R, Yagihashi S, Takahashi K, Fukuzawa M, et al. Inhibition of development of peripheral neuropathy in streptozotocin-induced diabetic rats with N-acetylcysteine. Diabetologia 1996;39:263–9.

[32] Drel VR, Lupachyk S, Shevalye H, Vareniuk I, Xu W, Zhang J, et al. New therapeutic and biomarker discovery for peripheral diabetic neuropathy: PARP inhibitor, nitrotyrosine, and tumor necrosis factor-{alpha}. Endocrinology 2010;151:2547–55.
[33] Obrosova IG, Pacher P, Szabó C, Zsengeller Z, Hirooka H, Stevens MJ, et al. Aldose reductase inhibition counteracts oxidative–nitrosative stress and poly(ADP-ribose) polymerase activation in tissue sites for diabetes complications. Diabetes 2005;54:234–42.
[34] Kuzumoto Y, Kusunoki S, Kato N, Kihara M, Low PA. Effect of the aldose reductase inhibitor fidarestat on experimental diabetic neuropathy in the rat. Diabetologia 2006;49:3085–93.
[35] Askwith T, Zeng W, Eggo MC, Stevens MJ. Oxidative stress and dysregulation of the taurine transporter in high-glucose-exposed human Schwann cells: implications for pathogenesis of diabetic neuropathy. Am J Physiol Endocrinol Metab 2009;297:E620–8.
[36] Hounsom L, Corder R, Patel J, Tomlinson DR. Oxidative stress participates in the breakdown of neuronal phenotype in experimental diabetic neuropathy. Diabetologia 2001;44:424–8.
[37] Hall KE, Sima AA, Wiley JW. Voltage-dependent calcium currents are enhanced in dorsal root ganglion neurones from the Bio Bred/Worchester diabetic rat. J Physiol 1995;486:313–22.
[38] Natarajan R, Nadler JL. Lipoxygenases and lipid signaling in vascular cells in diabetes. Front Biosci 2003;8:s783–95.
[39] Natarajan R, Nadler JL. Lipid inflammatory mediators in diabetic vascular disease. Arterioscler Thromb Vasc Biol 2004;24:1542–8.
[40] Purves T, Middlemas A, Agthong S, Jude EB, Boulton AJ, Fernyhough P, et al. A role for mitogen-activated protein kinases in the etiology of diabetic neuropathy. FASEB J 2001;15:2508–14.
[41] Stavniichuk R, Drel VR, Shevalye H, Maksimchyk Y, Kuchmerovska TM, Nadler JL, et al. Baicalein alleviates diabetic peripheral neuropathy through inhibition of oxidative–nitrosative stress and p38 MAPK activation. Exp Neurol 2011;230:106–13.
[42] Obrosova IG, Li F, Abatan OI, Forsell MA, Komjáti K, Pacher P, et al. Role of poly(ADP-ribose) polymerase activation in diabetic neuropathy. Diabetes 2004;53:711–20.
[43] Sun D, Funk CD. Disruption of 12/15-lipoxygenase expression in peritoneal macrophages. Enhanced utilization of the 5-lipoxygenase pathway and diminished oxidation of low density lipoprotein. J Biol Chem 1996;271:24055–62.
[44] Nunemaker CS, Chen M, Pei H, Kimble SD, Keller SR, Carter JD, et al. 12-Lipoxygenase-knockout mice are resistant to inflammatory effects of obesity induced by Western diet. Am J Physiol Endocrinol Metab 2008;295:E1065–7.
[45] Obrosova IG, Stevens MJ. Effect of dietary taurine supplementation on GSH and NAD(P)-redox status, lipid peroxidation, and energy metabolism in diabetic precataractous lens. Invest Ophthalmol Vis Sci 1999;40:680–8.
[46] Cameron NE, Cotter MA, Basso M, Hohman TC. Comparison of the effects of inhibitors of aldose reductase and sorbitol dehydrogenase on neurovascular function, nerve conduction and tissue polyol pathway metabolites in streptozotocin-diabetic rats. Diabetologia 1997;40:271–81.
[47] Greene DA, Arezzo JC, Brown MB. Effect of aldose reductase inhibition on nerve conduction and morphometry in diabetic neuropathy. Zenarestat Study Group. Neurology 1999;53:580–91.
[48] Hotta N, Toyota T, Matsuoka K, Shigeta Y, Kikkawa R, Kaneko T, et al. Clinical efficacy of fidarestat, a novel aldose reductase inhibitor, for diabetic peripheral neuropathy: a 52-week multicenter placebo-controlled double-blind parallel group study. Diabetes Care 2001;24:1776–82.
[49] Hotta N, Akanuma Y, Kawamori R, Matsuoka K, Oka Y, Shichiri M, et al. Long-term clinical effects of epalrestat, an aldose reductase inhibitor, on diabetic peripheral neuropathy: the 3-year, multicenter, comparative Aldose Reductase Inhibitor-Diabetes Complications Trial. Diabetes Care 2006;29:1538–44.
[50] Jiang Y, Calcutt NA, Ramos KM, Mizisin AP. Novel sites of aldose reductase immunolocalization in normal and streptozotocin-diabetic rats. J Peripher Nerv Syst 2006;11:274–85.
[51] Uehara K, Yamagishi S, Otsuki S, Chin S, Yagihashi S. Effects of polyol pathway hyperactivity on protein kinase C activity, nociceptive peptide expression, and neuronal structure in dorsal root ganglia in diabetic mice. Diabetes 2004;53:3239–47.
[52] Shimoshige Y, Minoura K, Matsuoka N, Takakura S, Mutoh S, Kamijo M. Thirteen-month inhibition of aldose reductase by zenarestat prevents morphological abnormalities in the dorsal root ganglia of streptozotocin-induced diabetic rats. Brain Res 2009;1247:182–7.
[53] Shimoshige Y, Enomoto R, Aoki T, Matsuoka N, Kaneko S. The involvement of aldose reductase in alterations to neurotrophin receptors and neuronal cytoskeletal protein mRNA levels in the dorsal root ganglion of streptozotocin-induced diabetic rats. Biol Pharm Bull 2010;33:67–71.
[54] Ohi T, Saita K, Furukawa S, Ohta M, Hayashi K, Matsukura S. Therapeutic effects of aldose reductase inhibitor on experimental diabetic neuropathy through synthesis/secretion of nerve growth factor. Exp Neurol 1998;151:215–20.
[55] Ramos KM, Jiang Y, Svensson CI, Calcutt NA. Pathogenesis of spinally mediated hyperalgesia in diabetes. Diabetes 2007;56:1569–76.
[56] Nishikawa T, Edelstein D, Du XL, Yamagishi S, Matsumura T, Kaneda Y, et al. Normalizing mitochondrial superoxide production blocks three pathways of hyperglycaemic damage. Nature 2000;404:787–90.
[57] Stevens MJ, Lattimer SA, Kamijo M, Van Huysen C, Sima AA, Greene DA. Osmotically-induced nerve taurine depletion and the compatible osmolyte hypothesis in experimental diabetic neuropathy in the rat. Diabetologia 1993;36:608–14.
[58] Obrosova IG, Drel VR, Pacher P, Ilnytska O, Wang ZQ, Stevens MJ, et al. Oxidative–nitrosative stress and poly(ADP-ribose) polymerase (PARP) activation in experimental diabetic neuropathy: the relation is revisited. Diabetes 2005;54:3435–41.
[59] Lupachyk S, Shevalye H, Maksimchyk Y, Drel VR, Obrosova IG. PARP inhibition alleviates diabetes-induced systemic oxidative stress and neural tissue 4-hydroxynonenal adduct accumulation: correlation with peripheral nerve function. Free Radic Biol Med 2011;50:1400–9.
[60] Price SA, Gardiner NJ, Duran-Jimenez B, Zeef LA, Obrosova IG, Tomlinson DR. Thioredoxin interacting protein is increased in sensory neurons in experimental diabetes. Brain Res 2006;1116:206–14.
[61] Ido Y, Nyengaard JR, Chang K, Tilton RG, Kilo C, Mylari BL, et al. Early neural and vascular dysfunctions in diabetic rats are largely sequelae of increased sorbitol oxidation. Antioxid Redox Signal 2010;12:39–51.
[62] Akude E, Zherebitskaya E, Chowdhury SK, Smith DR, Dobrowsky RT, Fernyhough P. Diminished superoxide generation is associated with respiratory chain dysfunction and changes in the mitochondrial proteome of sensory neurons from diabetic rats. Diabetes 2011;60:288–97.
[63] Ng TF, Lee FK, Song ZT, Calcutt NA, Lee AY, Chung SS, et al. Effects of sorbitol dehydrogenase deficiency on nerve conduction in experimental diabetic mice. Diabetes 1998;47:961–6.
[64] Geisen K, Utz R, Grötsch H, Lang HJ, Nimmesgern H. Sorbitol-accumulating pyrimidine derivatives. Arzneimittelforschung 1994;44:1032–43.
[65] Obrosova IG, Fathallah L, Lang HJ, Greene DA. Evaluation of a sorbitol dehydrogenase inhibitor on diabetic peripheral nerve metabolism: a prevention study. Diabetologia 1999;42:1187–94.
[66] Suzuki T, Sekido H, Kato N, Nakayama Y, Yabe-Nishimura C. Neurotrophin-3-induced production of nerve growth factor is suppressed in Schwann cells exposed to high glucose: involvement of the polyol pathway. J Neurochem 2004;91:1430–8.
[67] Ramana KV, Tammali R, Reddy AB, Bhatnagar A, Srivastava SK. Aldose reductase-regulated tumor necrosis factor-alpha production is essential for high glucose-induced vascular smooth muscle cell growth. Endocrinology 2007;148:4371–84.
[68] Middlemas AB, Agthong S, Tomlinson DR. Phosphorylation of c-Jun N-terminal kinase (JNK) in sensory neurones of diabetic rats, with possible effects on nerve conduction and neuropathic pain: prevention with an aldose reductase inhibitor. Diabetologia 2006;49:580–7.